FUNCTIONAL CAPABILITIES OF THE BREADBOARD MODEL OF SIDRA SATELLITE-BORNE INSTRUMENT

***O.V. Dudnik*[1]*, *M. Prieto*[2], *E.V. Kurbatov*[1], *S. Sanchez*[2], *K.G. Titov*[1], *J. Sylwester*[3], *S. Gburek*[3], *P. Podgórski*[3]**

[1] *V.N. Karazin Kharkov National University, Svobody Square, 4, 61022 Kharkov, Ukraine,*
E-mail: Oleksiy.V.Dudnik@univer.kharkov.ua;
[2] *Space Research Group, Alcala University, Alcala de Henares, Spain,*
E-mail: mpm@aut.uah.es, sebastian.sanchez@uah.es, pablo.parra@uah.es;
[3] *Solar Physics Division, Space Research Center, Kopernika str., 11, 51-622, Wroclaw, Poland,*
E-mail: js@cbk.pan.wroc.pl, sg@cbk.pan.wroc.pl, pp@cbk.pan.wroc.pl

(Received February 22, 2013)

This paper presents the structure, principles of operation and functional capabilities of the breadboard model of SIDRA compact satellite-borne instrument. SIDRA is intended for monitoring fluxes of high-energy charged particles under outer-space conditions. We present the reasons to develop a particle spectrometer and we list the main objectives to be achieved with the help of this instrument. The paper describes the major specifications of the analog and digital signal processing units of the breadboard model. A specially designed and developed data processing module based on the Actel ProAsic3E A3PE3000 FPGA is presented and compared with the all-in one digital processing signal board based on the Xilinx Spartan 3 XC3S1500 FPGA.

PACS: 29.30.Aj, 94.80.+g, 29.40.Wk, 29.85.Ca

1. INTRODUCTION

In the process of designing vehicle-borne equipment, engineers apply different methods for protecting the electronic and optical elements against the adverse effects of charged radiation. Despite this effort, news about failures of space vehicle devices or systems is continued to be received. For example, according to the GOES-15 geostationary satellite data, star sensors of the "Venus-Express" space probe were subject to the impact of charged radiation enhanced fluxes as a result of a solar flare on March 7, 2012. The decision taken by the Flight Control Group of the European Space Agency was to temporarily withdraw the sensors from operation and to maintain the spacecraft orientation with the help of gyroscopes [1]. Even more hurtful conditions may be encountered if the satellite is in a interplanetary mission, going into orbits close to the Sun like Solar Orbiter [2] or Interhelioprobe [3]. The mission trajectory will inevitably cross the CME (coronal mass ejections, once per 24h on average) and Solar Energetic Particle (SEP) clouds (once per week or month depending on the level of solar activity). During crossing, very high density of energetic particles, higher than in the magnetosphere, may cause damage to the instruments on board. These examples prove the need to provide for continuous monitoring of radiation environment in the outer near-Earth space with the aid of specialized instruments.

The experimental data on solar corona X-rays, which were obtained with the use of scientific equipment installed on some low Earth orbit satellites, contained information concerned with energy particle fluxes below Earth radiation belts and in the region of South Atlantic Anomaly (SAA)[4-6]. This was due to the fact that X-ray sensing elements are sensitive to secondary electromagnetic radiation resulting from interaction between space-origin primary electrons and space vehicle structural materials [7]. Hence, planning further scientific experiments to study variations of electromagnetic background and its separate lines in energy range 1...100 keV, not only in the solar corona, but also close to planets that have magnetic fields, calls for attendant continuous registration of high-energy particle fluxes. Miniaturized SIDRA-type particle detector [8] would be very useful for interplanetary missions, to support the X-ray instruments like ChemiX [9]. SIDRA would allow saving resources of such instruments and help to understand the particle-induced signal in the X-ray detectors.

In recent years new detecting systems used to record charged particle fluxes have been developed at a fast rate. In particular, application of organic scin-

*Corresponding author E-mail address: Oleksiy.V.Dudnik@univer.kharkov.ua

tillators based on p-terphenyl or stilbene, involving registration of light flashes, with use of silicon photo multipliers [10-12] as part of the unit of instrument detectors, will allow to reduce the number of layers in the telescopic system, when compared with the use of semiconductor detectors only. Highly integrated electronic systems for digital signal processing, such as microprocessors and Field-Programmable Gate Array (FPGA) enable to engineer sufficiently simple and, at the same time, quite efficient small-size instruments and devices intended for recording and transmitting data on fluxes of particles of different sorts and energies.

This paper describes the principles of operation of the analog and digital signals processing modules of the SIDRA (Space Instrument for Determination of RAdiation environment) prototype, SIDRA's conceptual design is described in [13-16]. Electrical parameters of the modules, comparative characteristics of the all-in-one digital signal processing board GR-XC3S-1500, and the special-design board SRG-A3P-v2 based on the ProAsic3E A3PE3000 FPGA are presented.

2. SCIENTIFIC PROBLEMS SOLVABLE WITH USE OF SIDRA INSTRUMENT

Joint analysis of the data obtained with the help of solar X-ray spectrophotometer SphinX and satellite-borne telescope of electrons and protons STEP-F, which were engineered by the Space Research Center of the Polish Academy of Sciences, and V.N. Karazin Kharkiv National University, respectively, and mounted on the board of the "CORONAS-Photon" satellite, showed a material difference in the characteristics of energy electron spectra in the region of the SAA, of the outer and inner radiation belts [17]. There is evidence that even in the case of weak geomagnetic storms at small altitudes there can be observed two inner electron radiation belts of the Earth [18]. In this case, the energy spectrum of the extra inner belt is considerably softer than the main spectrum. In addition, electron beams below the radiation belts at an altitude of $\sim$ 550 km bear an expressed anisotropic character as compared to nearly isotropic distribution of particle fluxes in the SAA regions at similar altitudes. However, the above results were obtained during a quiet solar period within a short time and need to be given a more precise definition and confirmation. Considering this fact, further study of dynamics of fluxes and energy electron spectra continues to be critical.

The nature of generation of electron micro-bursts in low and subequatorial latitudes below the Earth radiation belts, at altitudes of several hundreds kilometers from the Earth surface, remains practically unexplored. Thus, in August, 2009, the instrument STEP-F installed on board of "CORONAS-Photon" spacecraft recorded tens- and thousand-fold intensification of electrons, having energy up to $\sim$ 0.5 MeV in the form of short-time micro-bursts. Such micro-bursts were observed in those zones of the magnetosphere where they were not expected to be found on the models of distribution of charged radiation, i.e. in low latitudes and close to the equator in the areas being far from SAA.

Illustrated in Fig. 1 is the time dependence of density of electron fluxes, with energies E_e=0.18...0.51 MeV, at an altitude of $\sim$ 550 km, on August 9, 2009, during the time period from 09h:25m to 09h:58m of the Universal Time, Coordinated (UTC), with a time resolution of 2 s. The green line denotes geographical latitudes of the satellite's position when it moves. As it can be seen in Figure 1, during the period between two passing of the inner radiation belt in the Southern and Northern hemispheres, in the satellite orbit ascending node, the STEP-F instrument, when passing low-latitude and subequatorial zones, recorded intensive bursts of fluxes of electrons, having energies E_e=0.18...0.51 MeV. The maximum amplitudes of the bursts were comparable to the particle flux density in the inner belt and were mainly recorded in low latitudes of the Northern hemisphere.

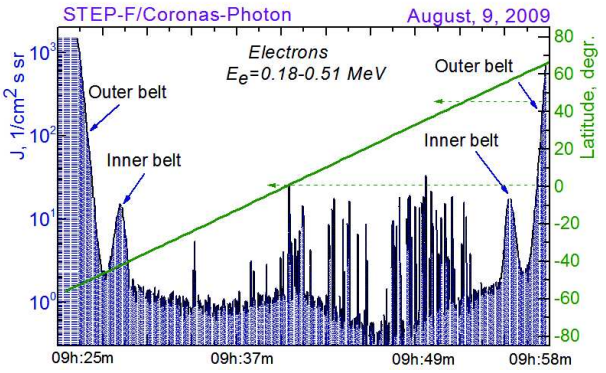

Fig.1. *Time dependence of electron flux density on August 9, 2009 with temporal resolution of 2 s, in the orbit ascending node, based on data of STEP-F instrument on board of "CORONAS-Photon" satellite. Right-hand scale of axis Y – geographical latitude of satellite position (green curve)*

With the consideration of the extremely low, constant level of solar X-ray emission and absence of geomagnetic activity at the time of measurements shown in Fig. 1, we postulate that such uncommon behavior of electrons might have been caused by an increased seismic activity and, in particular, by the earthquake of 7.1 magnitude near Japan at 10h:55m UTC, having coordinates of 33^0 northern latitude and 138^0 east longitude. To confirm this assumption and identify what are the reasons for the generation of intensive bursts of precipitating electrons in low latitudes and in the equatorial zone, there must be conducted further satellite experiments, involving a decrease in the lower energy registration threshold from E_e=180 keV to the minimum possible energy threshold.

3. INSTRUMENT COMPONENTS AND FUNCTIONAL UNITS

The designed and implemented instrument breadboard model [19] is shown in Fig. 2. The detector head is a telescopic structure consisting of 3 high-resistance silicon PIN-detectors of different thicknesses and an organic scintillation detector that has low values of effective charge and density. Located directly below the detector head is an analog signal processing module. The module consists of 3 single-type channels, comprising low-noise charge-sensitive preamplifiers (CSA), shaping amplifiers (ShA), scaling amplifiers (SCA), programmable-adjusted gain coefficients, as well as an separated ShA-based channel. Additionally, the 1^{st}, 2^{nd} and 3^{rd} signal processing channels comprise sample and hold circuits (S/H), as well fast-response analog-to-digital converters (ADCs). The principal tasks fulfilled by the signal digital processing module are the collection and primary processing of digital data provided by the ADCs, the identification of particles and their energies, and finally the transmission of the scientific data to the on-board computer [20].

Fig. 2. *General view of SIDRA instrument model*

The secondary power module is located in the lower part of the instrument and is designed as two identical semi-sets assembled on a common printed circuit board. The module operates in a «cold redundant» configuration. That is, only the semi-set that provides all secondary power supplies is connected to the on-board source of 18...36 V primary power. The other semi-set is disconnected, thus allowing the extension of the operational active time of the instrument. Protecting circuits are provided in both primary and secondary supply modules. The connected semi-set is selected by sending an appropriate telecommand. The status of all secondary voltage of both semi-sets is included in the satellite's telemetry system.

4. DETECTOR HEAD AND ANALOG SIGNAL PROCESSING MODULE

The detector head PIN-detectors are made of superpurity silicon and were produced on a special order by Micron Semiconductor, Ltd*. They are protected against direct sun rays and low-energy magnetospheric particles and interplanetary plasma with ~ 20 μm-thick aluminum foil. Such level of protection provides a threshold of E_e ≈40 keV for the low energy electrons.

Fig. 3 shows a general view of the detector head and silicon detectors enclosed in their mechanical cases. Fig. 4 shows the energy spectra of conversion electrons from β-radioactive source ^{207}Bi, which are recorded by means of detectors D2 and D3 with the use of conventional laboratory equipment under normal temperature and humidity conditions. The spectra demonstrate rather high effectiveness of data-recording for the maximum energy of E_e=1048 keV.

Fig. 3. *General view of detector head and silicon PIN-detectors*

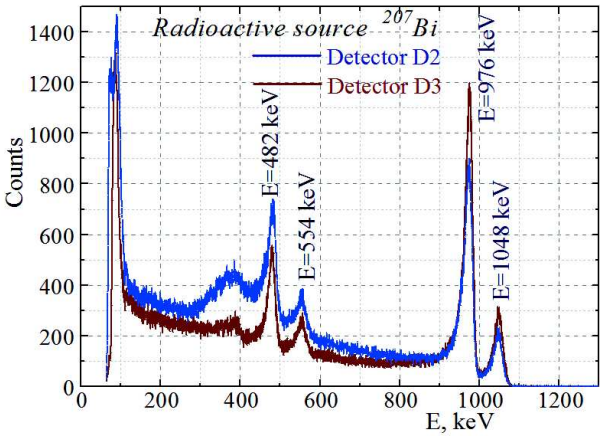

Fig. 4. *Energy spectra of β-radioactive source ^{207}Bi, which were recorded by detectors D2 and D3, having thickness values of 1 mm and 1.5 mm respectively*

*http://www.micronsemiconductor.co.uk

Table 1. *S_{CSA} sensitivity and ranges of recorded energies in respect of three values of gain coefficients G of scaling amplifiers, depending on feedback capacity C_f of CSA*

CSA			Shaper, U=25...3600 mV		
C_f, pF	S_{CSA}, mV/MeV	E_{max} at U_{out}=3.6V, MeV	ΔE at G_1=1, MeV	ΔE at G_2=10, MeV	ΔE at G_3=25, MeV
1	44.2	81.3	0.56...81.3	0.06...8.1	0.02...3.25
2	22.1	163	1.13...163	0.11...16.3	0.05...6.5
3	14.8	244	1.7...244	0.17...24.4	0.07...9.8
4.3	10.3	350	2.4...350	0.24...35	0.1...14.0
5.1	8.7	414	2.9...414	0.29...41.4	0.12...16.6
6.8	6.5	553	3.8...553	0.38...55.3	0.15...22.1
10	4.4	813	5.6...813	0.56...81.3	0.23...32.5

In respect of detector D3, the data-recording effectiveness is higher than in respect of D2. This is due to the larger thickness of the former and, consequently, a larger quantity of electrons that are completely stopped. The good energy resolution ranging from ΔE=14 keV to ΔE=17 keV in respect of electrons, having energies E_e=0.4...1 MeV, allows to construct the SIDRA instrument as a charged particle energy spectrometer providing an energy quantization step of $\Delta E \geq 20$ keV.

The charge-sensitive preamplifiers are based on broadband operational amplifiers. They include a feedback circuit where the feedback capacitance C_f determines the CSA sensitivity S_{CSA}, which is expressed in units mV/MeV. Table 1 presents the values of S_{CSA} and maximum possible recorded energies of particles at CSA outputs, depending on value C_f in those cases where CSA maximum output voltage is equal to U_{out} = 3.6 V.

The shaping amplifiers are based on an active band-pass filter together with baseline restoration circuits that function efficiently with the pulse repetition rate being up to f=250 kHz. The ShA gain coefficient is equal to 1.

The scaling amplifiers can modify the gain coefficients of the analog spectrometric channels by sending the appropriate commands from the on-board computer. In this case, the range of energies being recorded is changed. The ranges of recorded particle energies for three arbitrary values of gain coefficients of the scaling amplifier (G_1, G_2, G_3) are presented in Table 1. The range of output voltage values U=25...3600 mV corresponds to the linear part of characteristic U_{out}=f(U_{in}) of the S/H circuits of the analog signal processing spectrometric channels. The shaped pulse width amounts to ∼2.1 μs at level of 0.1 U_{max}, where U_{max} is the maximum amplitude of the output signals.

The sample and hold circuit has an extensive range of duration of signals for holding, low distortions, and allowing a maximum count rate up to f=600 kHz. The slew rate of peak detector signals is $W_{1,2,3}$=8.1 V/μs.

Each channel of the analog signal processing module has a test input that allows injecting test charge at the CSA input and observe the output signal of the shapers and peak detectors on the oscilloscope during the process of instrument adjustment.

5. DIGITAL SIGNAL PROCESSING MODULE

The diagram of Fig. 5 shows the main components of the digital signal processing module. It includes the FPGA that contains the LEON2 soft-processor, a software test debugging port, interfaces intended for connection with analog electronic equipment and on-board data collection subsystems.

For the development of the first prototype of the digital electronics module, and in order to reduce time and cost, a commercial version of the GR-XC3S-1500 board was used. This board was engineered by «Aeroflex Gaisler[†] and «Pender electronic design GmbH»[‡] companies. The software tools were written in C++ programming language and loaded via the RTEMS real-time operating system. The software enables to carry out routine data analysis in such a manner that a type of particle, its energy and flux density can be identified. Those requirements cause the microprocessor to perform a sequence of mathematical operations in real time.

The digital electronics prototype provides the two main input/output interfaces, the interface used for connection with the personal computer for debugging and testing purposes, and the interface used for connection with the analog electronic module. The computer interface is a 10/100 Mbit/s Ethernet link. Using the Ethernet port, the computer receives and stores the telemetry data generated by the instrument (scientific information and status data). It also sends commands and configures the instrument according to a chosen mode of operation. For operating the instrument, provisions are made to allow remote control in those cases where the instrument is connected to the Internet network. The main functions associated to the interface with the analog signal processing module are to collect data from the high-speed ADCs

[†]http//www.gaisler.com
[‡]http://www.pender.ch

and to analyze the S/H statuses. The later signals are used in the process of assessment of particle sorts in the real-time. Finally, some parameters of the analog electronics units can be adjusted, such as gain coefficients of the scaling amplifiers and discrimination threshold levels.

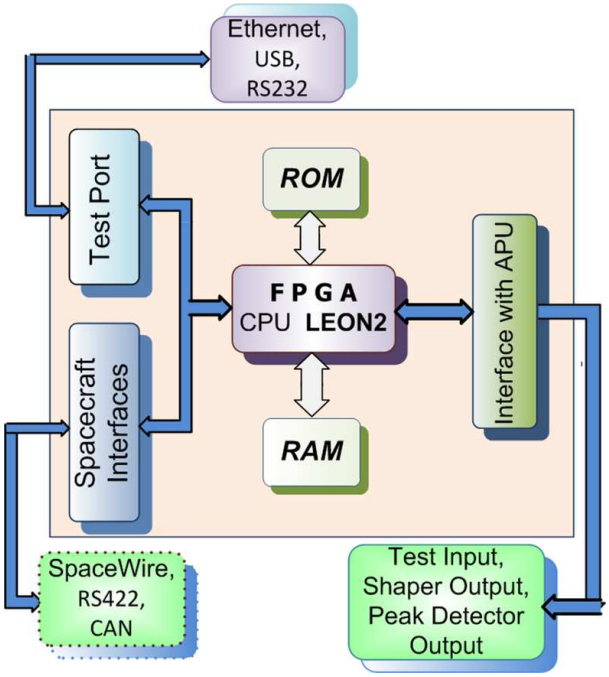

Fig.5. *Block-scheme of the digital signal processing module of SIDRA instrument prototype*

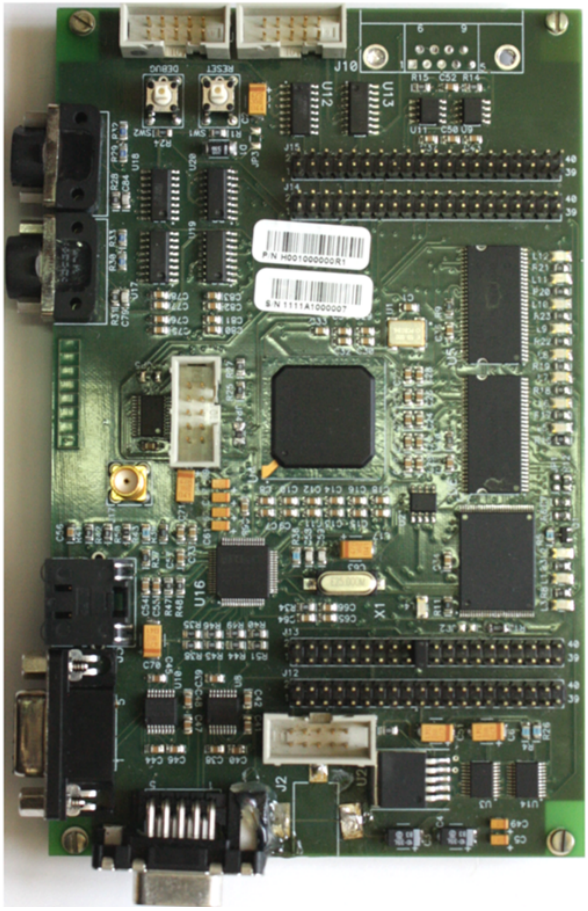

Fig.6. *General view of the SRG-A3P-v2 signal digital processing board of SIDRA instrument prototype*

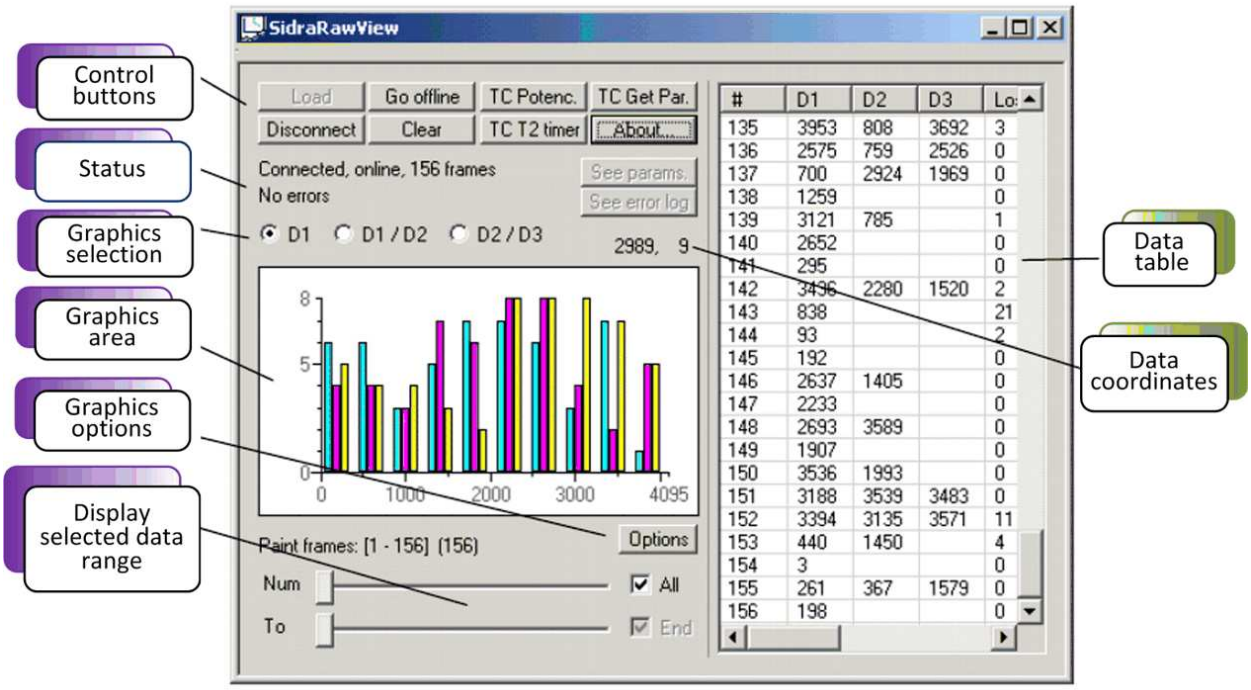

Fig.7. *View of the SidraRawView.exe program interface for reception and presentation of data in digital and graphic formats*

Table 2. *Comparative characteristics of the digital signal processing boards for SIDRA breadboard models*

Board	SRG-A3P-v2	GR-XC3S-1500
FPGA manufacturer	Microsemi SoC Products Group (former Actel)	Xilinx
FPGA type	ProAsic3E A3PE3000-FG484	Spartan 3 XC3S1500 4FG456
Main characteristics of FPGA		
Number of system gates	3 000 000	1 500 000
Number of logic cells	75 264	29 952
RAM, kbit	504	576
Flash ROM, bit	1 024	No
Maximal number of user I/O lines	341	333
Maximal clock rate, MHz	350	300
Input voltage,V	+5	+5
Secondary voltages on the board, V	+3,3; +2,5; +1,5	+3,3; +2,5; +1,2
Clock oscilator friquencies, MHz	50; 25	50; 25
Memory		
ROM	Flash 8 Mbytes	Flash 8 Mbytes
RAM	64 Mbytes PC-133 compatible	64 Mbytes PC-133 compatible
RAM expansion capacity	Up to 64 Mbytes x 64 bit on SODIMM-144	No
Interfaces		
RS-232 UARTs	2	2
RS-422 UARTs	4	No
Ethernet	10/100 Mbit	10/100 Mbit
SpaceWire	2 x LVDS	No
CAN bus	1 Dual	No
USB 2.0	No	1
ADC	AD7472	No
User input-output lines		
Number of differential lines	12 (LVDS (2,5V))	12 (LVDS (2,5V))
Number of general -purpose lines	60 (LVTTL/LVCMOS (3.3V))	60 (LVTTL/LVCMOS (3.3V))
Communication lins with complementary periphery	No	1 port 16 bit LVTTL/LVCMOS (3.3V)
Maximal line frequency, MHz	66	66
Dimensions, mm	100 x 160	100 x 160
Recomended soft CPU cores	Leon 2/3 is supported Leon 4	Leon 2/3 is supported Leon 4

The next stage of the development of the signal digital processing module involved the design of a new original board known as SRG-A3P-v2, which is plug-compatible with the above-mentioned GR-XC3S-1500 board. Figure 6 presents a general view of the SRG-A3P-v2 board. The major distinctive feature of the new board is the use of the Actel ProAsic3E A3PE3000 FPGA instead of Xilinx Spartan 3 XC3S1500 FPGA. Presented in Table 2 are the comparative characteristics of both digital signal processing boards. The advantages of the SRG-A3P-v2 board over an extensive range of parameters are evident.

The software tools to collect data and transmit to the control compute were developed in the C++ programming language. The SidraRawView.exe program is able to display data in real time, thus aiding in detecting anomalies in the data collection process. The main interface window of the SidraRawView program is shown in Fig.7. As it can be seen, a user can send telecommands, receive and monitor raw data, using only this interface window.

CONCLUSIONS

The breadboard model of the SIDRA compact single-unit instrument manufactured to monitor charged high-energy particles under outer-space conditions has been presented. The measured parameters of the solid-state detectors and the analog signal processing module allow to use the instrument for the registration of fluxes and energy spectra of electrons, protons and nuclei of light elements. The initial use of the GR-XC3S-1500 board manufactured by the companies “Aeroflex Gaisler” and “Pender electronic design GmbH” in standard EuroCard form factor, including a Xilinx Spartan 3 FPGA and LEON2 soft-processor, allowed the prototyping of the data digital processing module. It also enabled to optimize the design and development of a new board based on the Actel ProAsic3E A3PE3000 FPGA. Based on it, the new laboratory model of the single-unit compact instrument, features small overall dimensions and low power consumption properties.

The work was carried out with the support of the Science-and-Technology Center in Ukraine, Grant No. 3542, University of Alcala, Grant No. CCG08-UAH/ESP-3991, and Ministry of Science and Innovations in Spain, Grant No. ESP2005-07290-C02-02.

References

1. O.V. Dudnik, M. Prieto, E.V. Kurbatov, S. Sanchez, T.G. Timakova, K.G. Titov, P. Parra. A Small-Sized Device for Monitoring of High-Energy Electrons and Nuclei in the Outer Space // *Space Scie. Technol.* 2012, v. 18, N6, p. 22-34 (in Russian).

2. W.I. Axford, E. Marsch, V.N. Oraevsky, V.D. Kuznetsov, T.K. Breus, et al. Space mission for exploration of the Sun, Mercury and inner heliosphere ("InterHelios") // *Adv. Space Res.* 1998, v. 21, N1-2, p. 275–289.

3. V.D. Kuznetsov, V.N. Oraevsky. Polar-Ecliptic Patrol (PEP) for Solar Studies and Monitoring of Space Weather // *Journ. British Interplanetary Soc.* 2002, v. 55, N11-12, p. 398-403.

4. A.S. Glyanenko, Yu.D. Kotov, A.V. Pavlov, A.I. Arkhangelsky, V.T. Samoilenko, V.N. Yurov, V.M. Pankov, S.P. Ryumin. The AVS-F experiment on recording rapidly changing fluxes of cosmic and gamma radiation prepared under the CORONAS-F project // *Instrum. Exper. Tech.* 2009, v. 42, N5, p. 596–603.

5. I.V. Arkhangelskaja, D.B. Amandjolova, A.I. Arkhangelsky, Yu.D. Kotov. Features of quasi-stationary precipitations according to the data obtained with the AVS-F instrument onboard the CORONAS-F satellite // *Solar Syst. Res.* 2008, v. 42, N6, p. 536–542.

6. O.V. Dudnik, P. Podgorski, J. Sylwester, S. Gburek, M. Kowalinski, M. Siarkowski, S. Plocieniak, J. Bakala. Investigation of Electron Belts in the Earth's Magnetosphere with the Help of X-ray Spectrophotometer SphinX and Satellite Telescope of Electrons and Protons STEP-F: Preliminary Results // *Space Scie. Technol.* 2011, v. 17, N4, p. 14-25 (in Russian).

7. O.V. Dudnik, P. Podgorski, J. Sylwester, S. Gburek, M. Kowalinski, M. Siarkowski, S. Plocieniak, and J. Bakala. X-Ray Spectrophotometer SphinX and Particle Spectrometer STEP-F of the Satellite Experiment CORONAS-PHOTON. Preliminary Results of the Joint Data Analysis // *Solar Syst. Res.* 2012, v. 46, N2, p. 160–169.

8. O.V. Dudnik, V.K. Persikov, E.V. Kurbatov, Yu.D. Kotov, V.N. Yurov. Principles of elaboration for particle analyzer SIDRA of the "Solar monitor" project // *Scientific session of National Research Nuclear University "Moscow Engineering Physics Institute-2011".* Moscow, Russia. Abstracts. v. 2 "Fundamental problems of the science", p. 115 (in Russian).

9. J. Sylwester, J. Bakala, P. Podgórski, M. Kowaliński, Z. Kordylewski, S. Gburek, et al. ChemiX – New generation solar soft X-ray Bragg spectrometer // *in Proc. of workshop "INTERHELIOPROBE Project. Tarusa, 11–13 May 2011".* Moscow, IZMIRAN, Russia, Ed. V.D. Kuznetsov, p. 52-64 (in Russian).

10. D. Renker. Geiger-mode avalanche photodiodes, history, properties and problems // *Nucl. Instrum. Meth. A.*2006, v.567, iss. 1, p. 48-56.

11. A. Vacheret, G.J. Barker, M. Dziewiecki, P. Guzowski, M.D. Haigh, B. Hartfiel, A. Izmaylov, et. al. Characterization and simulation of the response of Multi-Pixel Photon Counters to low light levels // *Nucl. Instrum. Meth. A.* 2011, v. 656, iss. 1, p. 69-83.

12. S. Korpar. Status and perspectives of solid state photon detectors // *Nucl. Instrum. Meth. A.* 2011, v. 639, iss. 1, p. 88-93.

13. O.V. Dotsenko, O.V. Dudnik, D. Meziat, M. Prieto. Concept of application of the SIDRA instrument to ensure safe operation of a satellite // *9th Ukrainian Conf. on space research.* Crimea, Ukraine. Abstracts, 2009, p. 76.

14. O.V. Dudnik, D. Meziat, M. Prieto. The concept of compact on-board instrument for measurements of particle fluxes and dose rates // *Scientific Session of Moscow Engineering Physics Institute-2009*, Moscow, Russia, Abstracts. 2009, v. 2. p. 151 (in Russian).

15. O.V. Dudnik, V.V. Bilogub, E.V. Kurbatov, et. al. Compact on-board instrument SIDRA for measurement of particle fluxes and dose rates – concept and first model // *9th Ukrainian Conf. on space research.* Crimea, Ukraine. Abstracts, 2009, p. 78.

16. O.V. Dudnik, M. Prieto, E.V. Kurbatov, S. Sanchez, T.G. Timakova, V.N. Dubina, P. Parra. First concept of compact instrument SIDRA for measurements of particle fluxes in the space // *Journ. of Kharkiv University, phys. series "Nuclei, Particles, Fields".* 2011, v. 969, iss. 3(51), p. 62-66.

17. P. Podgorski, O.V. Dudnik, J. Sylwester, S. Gburek, M. Kowalinski, M. Siarkowski, S. Plocieniak, J. Bakala. Joint analysis of SphinX and STEP-F instruments data on magnetospheric electron flux dynamics at low Earth orbit // *39th Scientific Assembly of the Committee on Space Research, July 14-22, 2012.*

Mysore, India. Abstracts. Panel PSW.3: "Space Weather Data: Observations and Exploitation for Research and Applications". STW-C-119 PSW.3-0028-12. p. 112.

18. Oleksiy Dudnik. Unexpected behavior of subrelativistic electron fluxes under Earth radiation belts // *4th Int. workshop HEPPA/SOLARIS-2012, 9-12 October 2012.* Boulder, Colorado, USA. Abstract book, p. 15.

19. O.V. Dudnik, S. Sanchez, M. Prieto, E.V. Kurbatov, T.G. Timakova, V.N. Dubina, P. Parra. Onboard instrument SIDRA prototype for measurements of radiation environment in the space // *39th Scientific Assembly of the Committee on Space Research. July 14-22, 2012.* Mysore, India. Abstracts. Session H0.3: "Technical Development of Instrumentation for Current Missions", STW-B-153 H0.3-0023-12, p. 106.

20. M. Prieto, D. Guzman, J.I. Garcia, et. al. Control Unit of the SIDRA Scientific Instrument // *Proc. of 9th Conf. "Jornadas de Computacion Reconfigurable y Aplicaciones".* Alcala de Henares, Spain. 2009, p. 475-484.

ФУНКЦИОНАЛЬНЫЕ ВОЗМОЖНОСТИ ЛАБОРАТОРНОГО МАКЕТА СПУТНИКОВОГО ПРИБОРА SIDRA

А.В. Дудник, М. Прето, Е.В. Курбатов, С. Санчез, К.Г. Титов, Я. Сильвестер, Ш. Гбурек, П. Подгурски

Представлены структурная схема, принципы работы и функциональные возможности лабораторного макета компактного спутникового прибора SIDRA, предназначенного для мониторинга потоков заряженных частиц высоких энергий в космическом пространстве. Обосновывается необходимость разработки спектрометра частиц и приводится перечень актуальных задач, решаемых с помощью прибора. Представлены основные характеристики узлов аналоговой и цифровой обработок сигналов лабораторного прототипа. Специально разработанный и изготовленный модуль обработки данных на основе ПЛИС Actel ProAsic3E A3PE3000 представлен в сравнении с универсальной платой цифровой обработки сигналов на основе ПЛИС XilinX Spartan 3 XC3S1500.

ФУНКЦІОНАЛЬНІ МОЖЛИВОСТІ ЛАБОРАТОРНОГО МАКЕТУ СУПУТНИКОВОГО ПРИЛАДУ SIDRA

О.В. Дудник, М. Прето, Є.В. Курбатов, С. Санчез, К.Г. Тітов, Я. Сільвестер, Ш. Гбурек, П. Подгурскі

Представлено структурна схема, принципи роботи і функціональні можливості лабораторного макету компактного супутникового приладу SIDRA, призначеного для моніторингу потоків заряджених частинок високих енергій у космічному просторі. Обґрунтовується необхідність розробки спектрометру частинок й наводиться перелік актуальних здач, що можуть вирішуватись за допомогою приладу. Представлено основні характеристики вузлів аналогової і цифрової обробки сигналів лабораторного прототипу. Спеціально розроблений і виготовлений модуль обробки даних на основі ПЛІС Actel ProAsic3E A3PE3000 представлений у порівнянні з універсальною платою цифрової обробки сигналів на основі ПЛІС XilinX Spartan 3 XC3S1500.